Developments of the off-plane x-ray grating spectrometer for IXO

R. L. McEntaffer, N. J. Murray, A. D. Holland, J. Tutt, S. J. Barber, et al.

R. L. McEntaffer, N. J. Murray, A. D. Holland, J. Tutt, S. J. Barber, R. Harriss, T. Schultz, S. Casement, C. Lillie, D. Dailey, T. Johnson, R. Danner, W. Cash, B. Zeiger, A. Shipley, M. Page, D. Walton, P. Pool, J. Endicott, D. Willingale, "Developments of the off-plane x-ray grating spectrometer for IXO," Proc. SPIE 7732, Space Telescopes and Instrumentation 2010: Ultraviolet to Gamma Ray, 77321K (29 July 2010); doi: 10.1117/12.857460

SPIE.

Event: SPIE Astronomical Telescopes + Instrumentation, 2010, San Diego, California, United States

Developments of the Off-Plane X-ray Grating Spectrometer for IXO

McEntaffer, R. L.*[a], Murray, N. J.[b], Holland, A. D.[b], Tutt, J.[b], Barber, S. J.[b], Harriss, R.[b], Schultz, T.[a], Casement, S.[c], Lillie, C.[c], Dailey, D.[c], Johnson, T.[c], Danner, R.[c], Cash, W.[d], Zeiger, B.[d], Shipley, A.[d], Page, M.[e], Walton, D.[e], Pool, P.[f], Endicott, J.[f], Willingale, D.[g]
[a] Dept. of Physics and Astronomy, University of Iowa, Iowa City, IA, USA 52240;
[b]Planetary and Space Sciences Research Inst., Open University, Milton Keynes, UK MK7 6AA
[c]Northrop Grumman Aerospace Systems, 1 Space Park, Redondo Beach, CA 90278, USA
[d]Ctr. for Astrophysics and Space Astronomy, University of Colorado, Boulder, CO, USA 80303
[e]Mullard Space Science Laboratory, University College London, Surrey, UK RH5 6NT
[f]e2v technologies plc, 106 Waterhouse Lane, Chelmsford, CM1 2QU, UK
[g]Dept. of Physics and Astronomy, University of Leicester, Leicester, UK LE1 7RH

ABSTRACT

The International X-ray Observatory (IXO) is a collaborative effort between NASA, ESA, and JAXA. The IXO science goals are heavily based on obtaining high quality X-ray spectra. In order to achieve this goal the science payload will incorporate an array of gratings for high resolution, high throughput spectroscopy at the lowest X-ray energies, 0.3 – 1.0 keV. The spectrometer will address a number of important astrophysical goals such as studying the dynamics of clusters of galaxies, determining how elements are created in the explosions of massive stars, and revealing most of the "normal" matter in the universe which is currently thought to be hidden in hot filaments of gas stretching between galaxies. We present here a mature design concept for an Off-Plane X-ray Grating Spectrometer (OP-XGS). This XGS concept has seen recent significant advancements in optical and mechanical design. We present here an analysis of how the baseline OP-XGS design fulfills the IXO science requirements for the XGS and the optical and mechanical details of this design.

Keywords: International X-ray Observatory, X-ray Grating Spectrometer, off-plane diffraction gratings

1. INTRODUCTION

The purpose of the OP-XGS is to provide high spectral resolution, $\lambda/\Delta\lambda > 3000$, and high effective area, > 1000 cm^2 at low energies, 0.3-1.0 keV. The spectrometer consists of an array of reflection gratings in the off-plane mount that diffracts light onto an array of dedicated CCDs[1, 2, 3, 4]. Light intersects the surface of the grating at grazing incidence, ~2.5°, and nearly parallel to the groove direction. This maximizes the illumination efficiency on the gratings. Furthermore, the groove profile can be blazed to preferentially diffract light to only one side of zero order thus increasing the efficiency further. The off-plane geometry leads to diffraction along an arc at the focal plane. A summary of the generic off-plane geometry is shown in Figure 1[5].

The viewing orientation for the diagram on the right is normal to the focal plane. Therefore, we are looking approximately down the optical axis. In this orientation the gratings are extending from the focal plane toward the observer. In reality, the gratings will not extend from their position in the spacecraft all the way to the focal plane, but this situation is shown here for illustrative purposes. The arrows emanating from the grating surface show two possible paths for a ray of light intersected by a grating. If the light was allowed to continue unimpeded by gratings, then it would propagate to the telescope focus which happens to lie in the grating focal plane along the circle defined by the arc

*randall-mcentaffer@uiowa.edu; phone 1 319 335-13007; fax 1 319 335-1753

Space Telescopes and Instrumentation 2010: Ultraviolet to Gamma Ray,
edited by Monique Arnaud, Stephen S. Murray, Tadayuki Takahashi, Proc. of SPIE Vol. 7732,
77321K · © 2010 SPIE · CCC code: 0277-786X/10/$18 · doi: 10.1117/12.857460

of diffraction. The dashed arrow shows specular reflection into zero order, which lies vertically displaced from the telescope focus, while the solid arrow depicts a diffracted beam on one side of zero order.

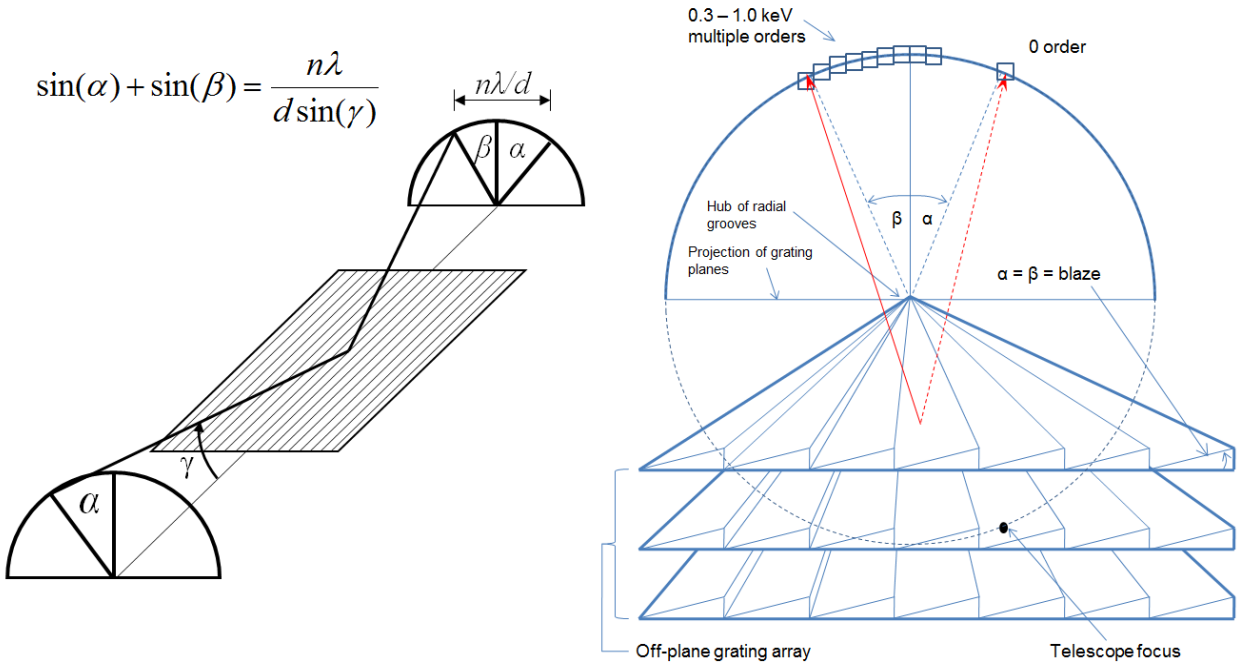

Figure 1. On the left an incoming ray of light intersects a grating in the off-plane mount with an azimuthal angle of α and graze angle of γ. Light is diffracted to an angle of β, dependent on wavelength and according to the grating equation. The diagram to the right shows the arc of diffraction at the focal plane and depicts several off-plane gratings placed in an array in order to collect light from some fraction of a telescope beam.

This diagram illustrates several of the key concepts that will be utilized for IXO. First, given the shallow graze angle necessary for efficient reflection of X-rays, several gratings will need to be placed into an array to capture the appropriate section of the telescope beam and ultimately achieve the required effective area. A small, representative section is shown in the figure. Second, this figure demonstrates the concept of blazing the grating grooves to maximize efficiency in only plus or minus orders. Third, the grating grooves will also exhibit a radial profile as opposed to typical parallel grooves. In order to maintain a constant graze angle over the array, the gratings are fanned such that the radial grooves of all gratings converge to a point on the focal plane denoted as the hub. This radial profile will match the convergence of the telescope beam which will maintain a consistent α over the array, thus nullifying any aberrations caused by the gratings. Therefore, the spectral resolution obtained by the gratings will be limited by the quality of the telescope. Spectral lines will have a width approximately equal to the half-energy width (HEW) of the telescope point spread function (PSF). However, the effective telescope PSF can be minimized by only sampling a fraction of the beam. Limiting the azimuthal coverage of the grating array, or in other words subaperturing, will decrease the width of the spectral lines thus increasing spectral resolution.

The high illumination efficiency combined with the use of a blazed grating ensure high throughput in diffracted orders. Furthermore, the use of radial profiles and the technique of subaperturing will maximize spectral resolution. In this way an off-plane reflection grating spectrometer will be able to meet the requirements for IXO. The design and results presented here were formulated during an ESA Instrument Study of IXO. Therefore, for analysis and configurations, Silicon Pore Optics (SPO) are considered as the telescope optics in the Fixed Mirror Assembly (FMA). However, much of this analysis is still applicable to a Slumped Glass FMA or any 20 m focal length optic.

The OP-XGS is comprised of two basic elements: 1) a grating system, and 2) a camera[6, 7, 8]. The grating system will consist of the grating array, structure to mount the gratings at the required position, and a thermal control system for the array. The camera will consist of an array of CCDs with associated electronics and thermal control. The OP-XGS can achieve the instrument performance requirements at any position along the optical axis from just aft of the optics to just a few meters away from the focal plane. Therefore, the parameter space available for placement of the gratings (and thus size of the gratings, structure, camera, etc.) is inherently large. An extensive trade study has therefore been undertaken. The results of this study favor what has been named the "tower" design, which consists of the grating array placed 5.16 m from the focal plane via the use of a structural tower[9, 10]. A nominal layout is illustrated in Figure 2.

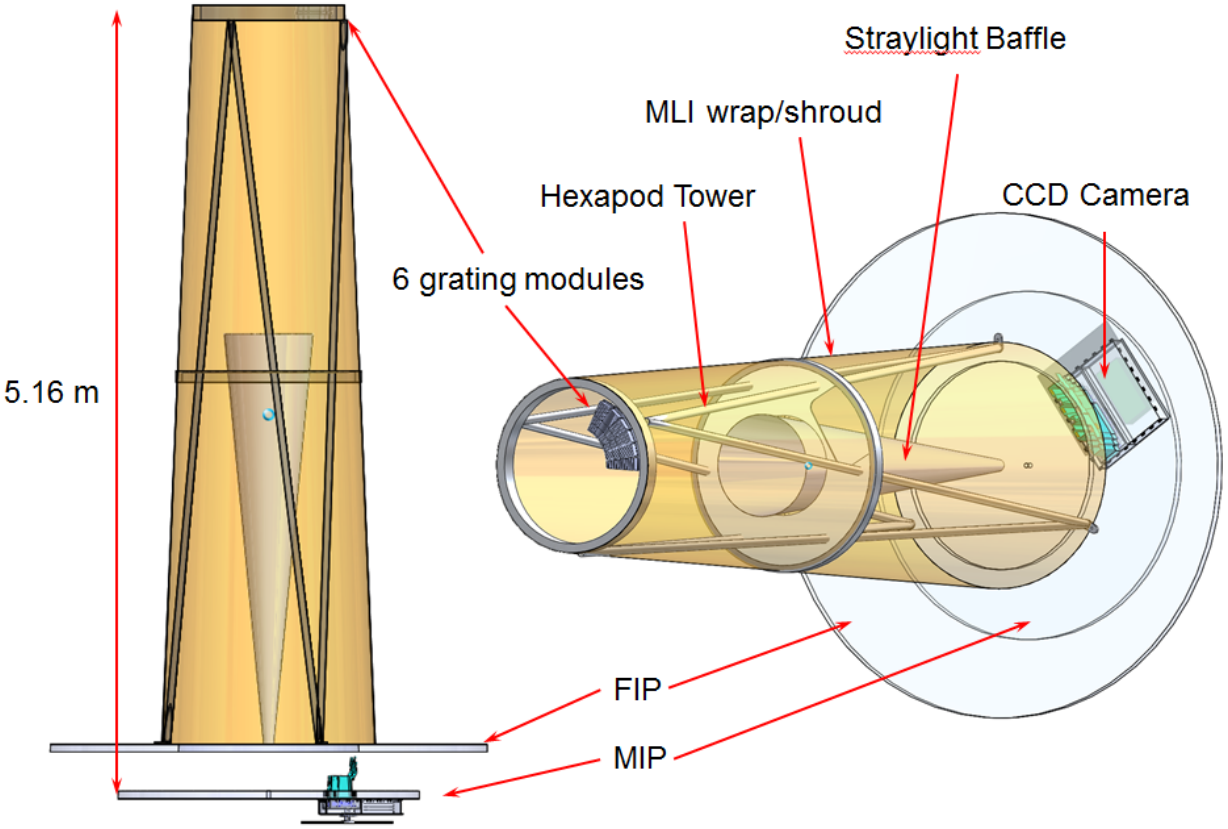

Figure 2. Nominal OP-XGS configuration. The gratings are mounted on a tower and located 5.16 m from a CCD camera at the focal plane.

The camera can be extended from the FIP or mounted to the XY-static portion of the MIP that is only adjusted in Z. The straylight baffle is not an OP-XGS required component, but shown here just for reference as such a baffle may be required by the observatory. The tower design can provide for structural support of several observatory system beneficial components such as this straylight baffle, magnetic diverters, and additional straylight protetion as depicted by the tower shroud shown in this figure.

Figure 3 displays a close-up view of one of the 6 grating modules. The size and shape of these modules (and the gratings within them) ultimately determines the effective area and resolution of the system. Verification of these requirements is performed using detailed raytrace analysis as described in the next section.

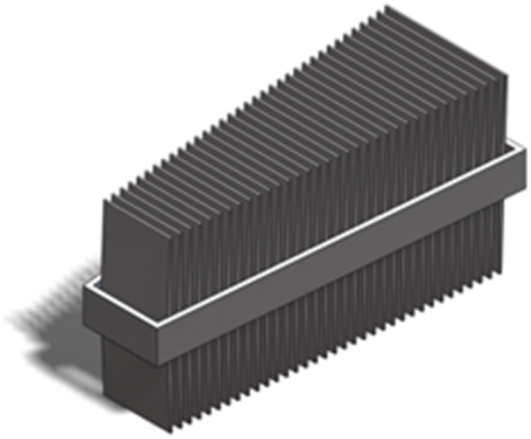

Figure 3. A single grating module.

2. OPTICAL DESIGN

The instrument optical design for OP-XGS is verified using detailed raytrace analysis. This analysis consists of using a collimated X-ray source feeding a representative set of telescope optics which provides a beam to the grating modules which disperse the X-rays onto the camera. The main parameters of the optical design are determined by the need to provide a grating array that can meet the performance requirements. This leads to restrictions on the grating module size (to obtain spectral resolution) which leads to necessitating a minimum number of modules (to obtain effective area). Even when limited to the tower position, the OP-XGS design still exhibits much flexibility and a large parameter space. Therefore, the final design was made to meet the science requirements while being possible to accommodate changes in the IXO spacecraft configuration and/or the requirements themselves as the spacecraft design evolves in subsequent phases.

The first requirement to consider is the effective area. The grating array needs to cover a requisite amount of the telescope beam to achieve >1000 cm^2 of total effective area when considering the throughput of the telescope, the throughput of the grating array and the QE of the CCDs. The analysis begins with characterization of these factors. Figure 4 shows the effective area of the SPO optics and the theoretical grating efficiency.

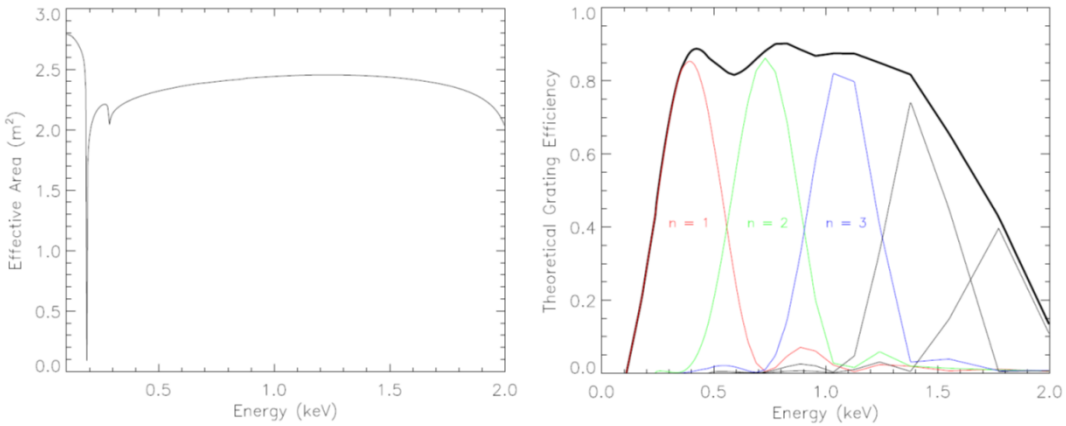

Figure 4. Left – SPO effective area including a 10% margin loss. Right – theoretical efficiency curves for multiple orders (n = 1-5) from a prototype grating. These values are derived from AFM measurements of the actual groove profile.

The effective area for the SPO has been calculated using document IXO_SPO_area_hires_B4C-coating_outerrow_35_2010030241.dat and the associated IXO_reference_design_35-rows.pdf. The optics have a 8 nm B4C coating over Ir. These telescope effective area estimates include a 10% margin loss due to particulate contamination and alignment losses. The grating efficiencies are derived from atomic force microscopy (AFM) measurements of a current prototype grating. Empirical results from similar gratings match well with the theoretical curves. Also considered is the mechanical throughput of the gratings which is 93%. This comes from a 150 mm long grating at 2.5° graze with a 0.5 mm thick edge.

Combining these throughputs for the 6 grating modules with the quantum efficiency (QE) of the CCDs results in the effective area curve shown in Figure 5. This curve obtains an average of 1519 cm^2 over the required energy band with a minimum of 1000 cm^2 at 0.3 keV. This curve also shows the possibility of extending the energy band up to 1.5 keV. This is particularly attractive given that these energies, in multiple orders, will already be collected by the CCDs. The limit at the low energy end is ultimately determined by the absorption of soft X-rays in the Si of the CCDs combined with the absorption effects of the optical blocking filter on the CCDs, 28 nm Al + 13 nm MgF_2.

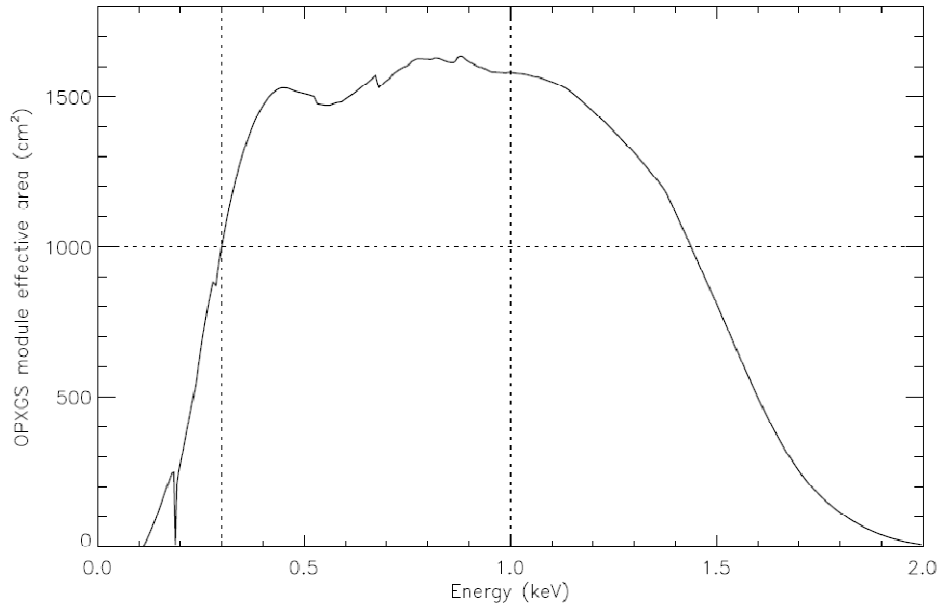

Figure 5. Total effective area for the OP-XGS.

Once the effective area has been achieved the spectral resolution is the next requirement to drive the design. High resolution is obtained by subaperturing the scatter function of the telescope optics. Limiting the azimuth of the gratings reduces the spot PSF in the dispersion direction thus increasing the resolution. However, unrecoverable image errors from contributions such as pointing jitter, system jitter, and metrology measurement errors limit the subaperture potential as these errors cannot be removed. If the telescope scatter is the only factor to consider, then the 11° azimuth grating modules give the spectral line shown on the left of Figure 6. In this raytrace the telescope HEW due to scatter is 4.7". The gratings limit this HEW to < 0.3" in the dispersion direction due to the supaperture effect.

The telescope beam will be dominated by scatter, but other factors will add to the HEW. These factors include pointing errors, telescope alignment errors, metrology errors, moisture release, 1-g release, thermo-elastic effects, and high frequency jitter. These errors cannot be decreased through the use of subaperturing and therefore may degrade the spectral resolution of the XGS. These errors contribute to a different degree and in different ways. Also, many of these errors include a static term and a dynamic term. For instance, metrology errors will consist of a telescope offset and an

error on the measurement of that number. As long as the offset is constant during an observation the static term does not effect spectral resolution, just the dynamic term, which is typically small in comparison. Another example is the pointing error. The accuracy to which the telescope can point to a certain RA and Dec is currently set to 1" (3σ radius). This does not effect spectral resolution, but how well the observatory can stay at that RA and Dec does effect the XGS. Therefore, spectral resolution is more concerned with the jitter in the pointing. Finally, many of the error terms (moisture release, 1-g release, thermo-elastic effects, metrology errors) can either be calibrated out or are slow in comparison to the sampling rate of the OP-XGS CCDs. A proper characterization of high frequency jitter needs to be performed to assess the effects on spectral resolution, but initial estimates place a low significance to this number.

The detailed raytrace is performed again with inclusion of the effects from these errors. The worst case scenario is considered to be 1" (3σ radius) pointing jitter and 1.2" (3σ radius) due to other factors. This gives an RSS total of 1.6" (3σ radius). The other case considered is an RSS total of 1" (3σ radius). These results are shown on the left and center of Figure 6, respectively.

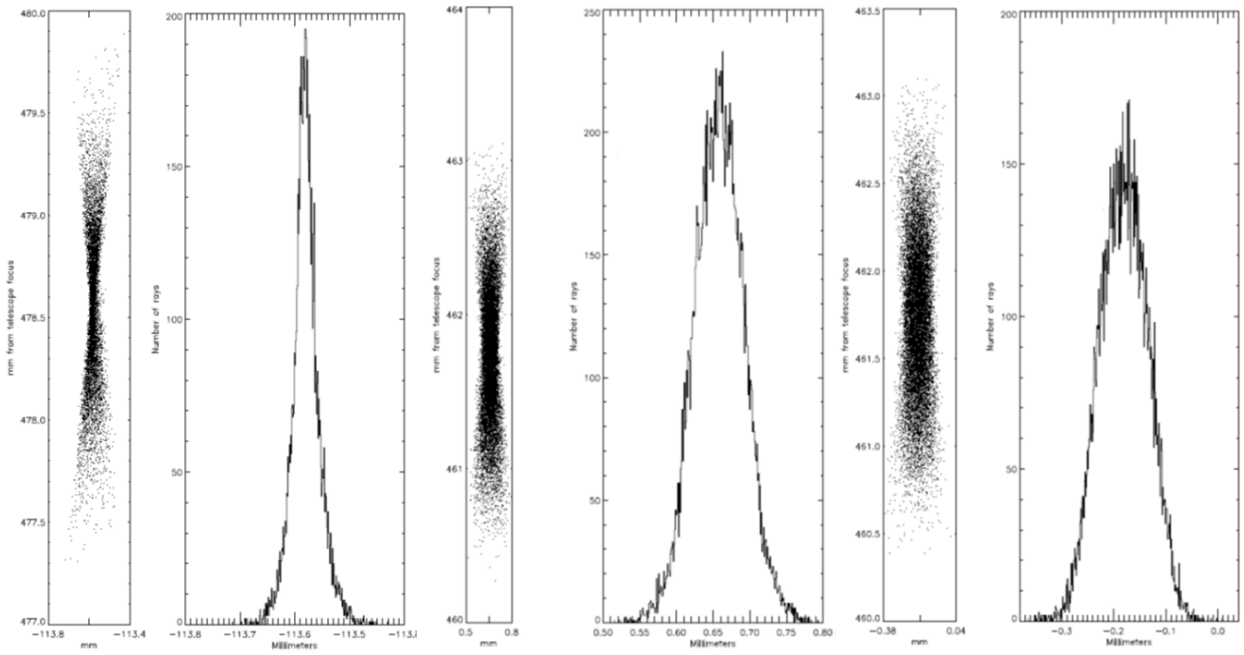

Figure 6. Left - Spectral line from a single grating module given a 4.7" HEW telescope beam. Center – The same telescope as on the left, but including a total of 1" image errors. Right – Same telescope again, but combined with a worst case 1.6" of unrecoverable image errors.

These raytraces show the effect that image errors have on the subapertured beam. The core of the spectral line PSF becomes broadened with increasing image error contributions, thus decreasing spectral resolution. Therefore, it is key to accurately assess the actual contribution from these effects. The worst case scenario (1.6") assumes that static effects (in 2-axes) are included in the total error number. This is excessively conservative given that the OP-XGS is only sensitive to the dynamic terms which are much smaller. Furthermore, given that the spectral resolution is determined from one dimension these 2-axes errors can typically be reduced by √2. Therefore, the actual error contribution is probably closer to 1" or even less. The resolution obtained from these differing scenarios is outlined in Figure 7.

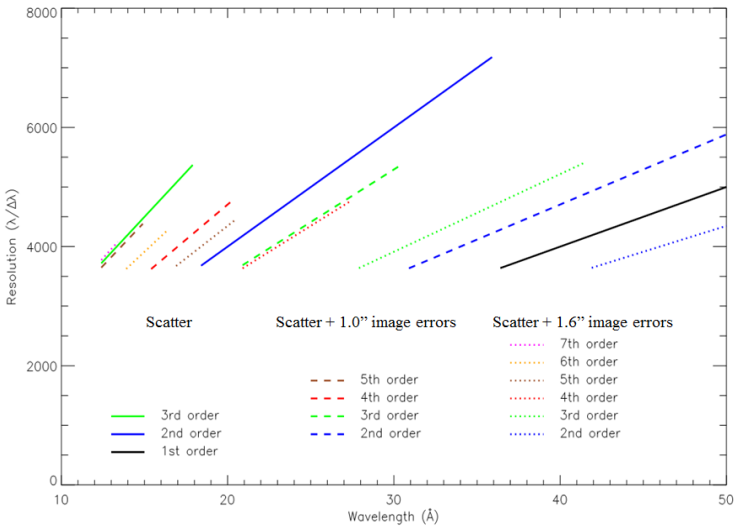

Figure 7: Resolution as a function of wavelength for a scatter dominated telescope (solid lines), the same telescope combined with 1" of unrecoverable image errors (dashed lines), and 1.6" of error (dotted lines).

The analysis was performed with a goal of building in a 20% margin. Therefore, spectral resolutions above 3600 (and upwards of 7200) are obtained over the energy band. This margin will be used to account for factors such as grating-to-grating alignment, grating surface errors, and other unforeseen errors. Figure 7 shows that given a scatter dominated telescope the OP-XGS will be able to obtain the required spectral resolution through the use of orders 1, 2, and 3. However, as image quality errors are introduced the spectral line width increases and the lower orders are no longer capable of obtaining the required resolution. This can be solved through the use of higher orders. In the 1.0" total error case orders 2-5 are necessary as shown by the dashed lines in Figure 7, while the 1.6" error case would require orders as high as 7. However, the use of higher orders necessitates coverage of much longer wavelengths, e.g. 7th order 1keV (12.4 Å) occurs at 86.8 Å, thus increasing the length of the CCD array. Therefore, the determination of the size and layour of the CCDs is determined by the spectral resolution, the impact of image errors, and the subsequent impact on the required bandpass. The final CCD layout determined from this analysis is shown in Figure 8.

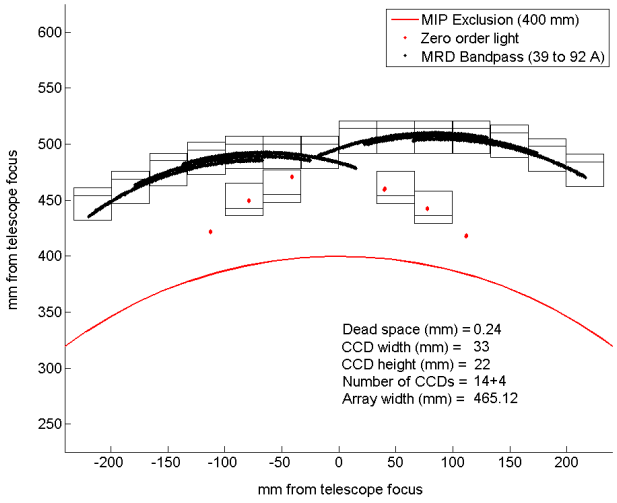

Figure 8: CCD layout determined by detailed raytrace of a 4.7" HEW subapertured telescope combined with up to 1.2" of image error. There are 6 individual spectra present corresponding to the 6 grating modules in the grating array.

The six grating modules disperse light into the six separate arcs and zero order locations as shown in Figure 8. Fourteen spectral CCDs (1-14) will be used to collect light in 2nd through 5th order (61 Å to 92 Å) to meet resolution requirements or, depending on tighter pointing tolerance and knowledge of image blur effects, the array can be reduced in size to the innermost ten CCDs and collect light in 1st through 3rd order (36 Å to 72 Å). Four extra CCDs will monitor the zero order reflections from the gratings to provide wavelength calibration. Both pairs of three arcs of dispersion are separated by 2 mm allowing each to be easily spatially resolved from one-another. Each arc falls no closer than 3 mm from the boundaries of the detectors in the array.

This layout is designed to be able to incorporate up to 1.2" of unrecoverable image errors, i.e. a conservative design providing for even greater margin on resolution. If image errors are determined to be more significant (e.g. 1.6") then the effective area requirement becomes affected. This can be remedied by adding an additional CCD to each end; however the likelihood of this eventuality is very low. The more likely scenario is that the image errors are a smaller factor than considered here. In this case the array could shrink by 2-4 CCDs as only the inner CCDs (lower orders) are utilized. Therefore, until a full analysis has been performed on the actual contribution of image errors to the OP-XGS spectral line width the design presented in Figure 8 will be considered the baseline and is predicted to be conservative.

Another feature of this CCD layout is that there are 6 individual spectra from the 6 modules in the grating array. These spectra fall at different positions on the CCD array and can be read independently. This is a benefit of the design providing spectral redundancy. Dead space between CCDs does not reduce the overall effective area below the requirement and loss of a CCD does not either, thus leading to the beneficial redundancy. Furthermore, tracking the zero order images at a high frame rate (~12 Hz) using 4 zero order monitors allows for further reduction in the impact from unrecoverable image errors. Given this CCD layout and an image error of 1.0", the contribution from each order to the overall spectrum can be determined. This is displayed in Figure 9.

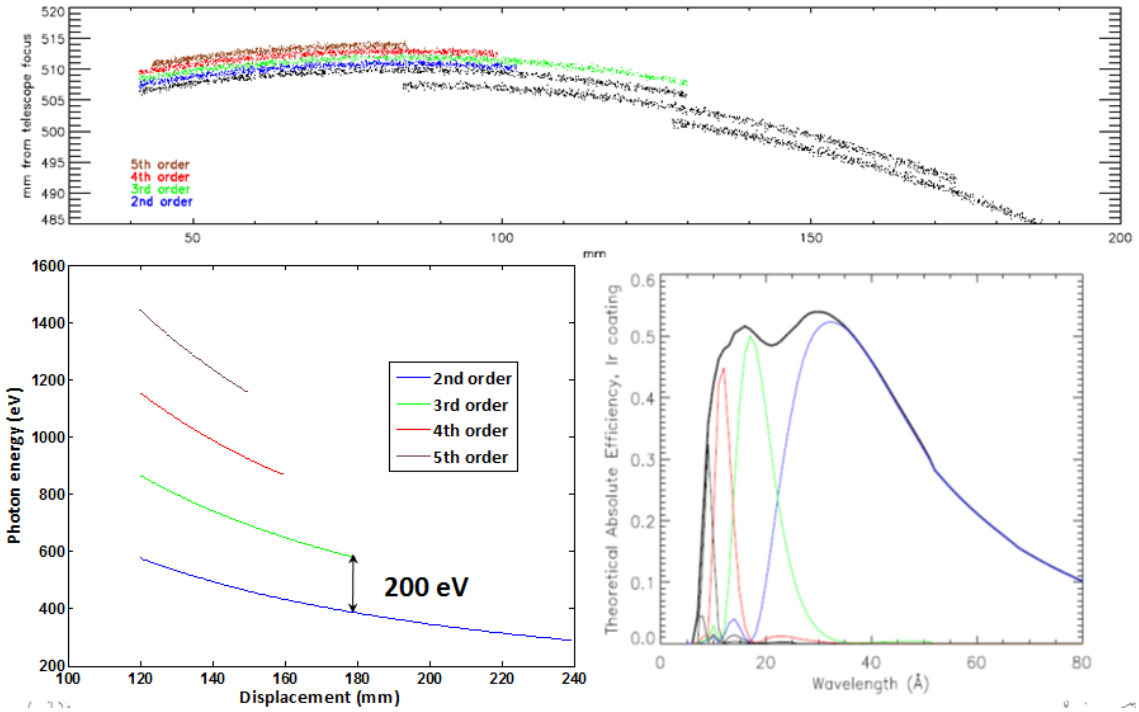

Figure 9. Spectral orders contained within a given spectrum. Top – the upper spectrum, shown in black, has its constituent orders separated by color and offset in the Y-axis for illustrative purposes. These same orders are shown at the bottom left as a function of energy giving a minimum gap of 200 eV.

The top image in Figure 9 shows roughly half of the CCD array, the right half shown in Figure 8. The black lines are raytraces of a continuous spectrum from 39-92 Å. The colored lines depict the spatial contribution to the upper spectrum for each order. The orders are offset in Y for illustrative purposes. The overlap of spectral orders drives the requirement for energy resolution at the CCD. The need for detecting orders 2-5 drive an energy resolution requirement of 200 eV as seen at the bottom-left of Figure 9. It is important to note that the orders maximized by the grating are dependent on the blaze angle on the gratings. Larger blaze angles will stretch the grating efficiency curve (lower right Figure 9) to the right thus including more orders in the efficiency curve allowing the use of higher orders. The final blaze angle on the gratings will be determined once the effects to image quality are quantified which will then determine CCD layout and necessary spectral orders.

The general instrument description combined with a detailed raytrace analysis that considers both effective area and spectral resolution are necessary exercises in determining the detailed mechanical designs of the grating array and the CCD camera. The thermal and electrical design follows from this as well. These are discussed in subsequent sections.

3. MECHANICAL DESIGN

3.1 Grating Array

The general layout of the 5.16 m tower design combined with detailed raytrace and effective area analyses lead to a detailed mechanical design of the gratings and camera. The design of the gratings are discussed here. For a discussion of the camera see Murray et al[6]. The grating array consists of 6 grating modules. Each of the 6 separate grating modules consists of 39 gratings in the off plane mount. Figure 10 shows the dimensions of one of the 6 grating modules.

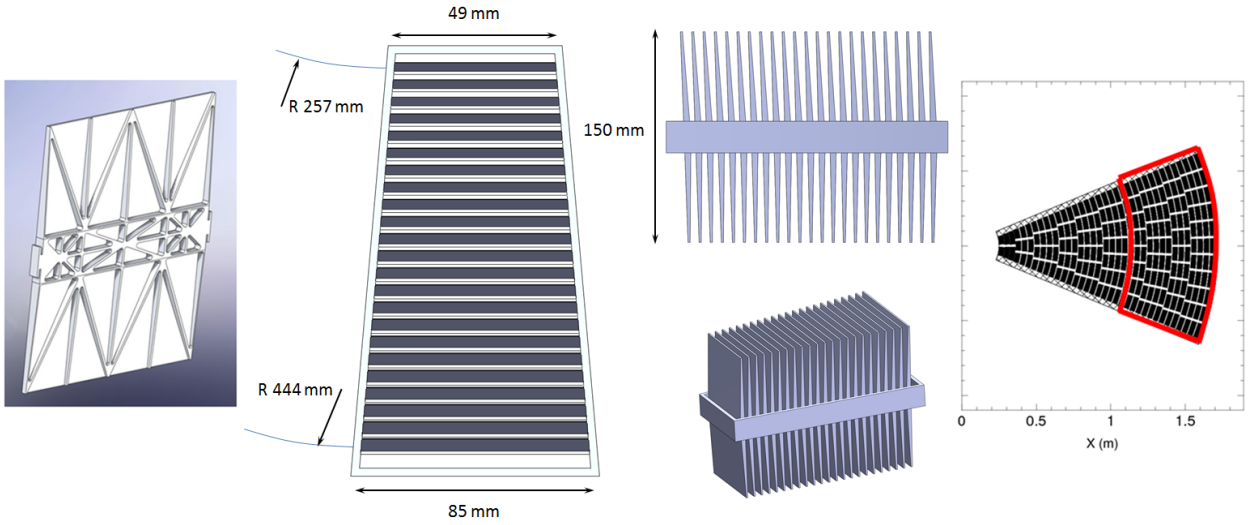

Figure 10. Left - Grating substrate CAD model. The substrate is made from Be and the back (non-optical) surface (shown) is lightweighted to save mass. The smooth optical surface is facing away. Center - Grating module design and dimensions. Right - Projection of the radial coverage of the grating array up to the SPO FMA.

The gratings begin with fabrication of Be substrates as shown on the left of Figure 10. The groove profile is then replicated onto the substrate using a holographically recorded master grating that has a radial groove profile that is subsequently ion etched to produce a blazed profile. The master is used to create a submaster which is then pressed into a thin epoxy layer applied to the substrate. When cured, the submaster is removed and the replicated grooves, which now resemble the master, are coated with Ir for high reflectivity in the required energy band. The substrates exhibit a trapezoidal profile when viewed from the side. This allows the gratings to be very thin at the edges, 0.5 mm, minimizing

losses due to the substrates themselves, but thick at their centers to maximize rigidity and surface figure quality. The groove dimension on each grating is 150 mm, roughly in the Z direction. This long groove length allows for increased mechanical throughput. The 0.5 mm edge thickness combined with the 150 mm groove length at a graze angle of 2.5° leads to a mechanical throughput of 93%.

After replication, the gratings are then aligned and epoxied within a "belly band" that secures small tabs located on the thick sections of the substrates. The resulting assembly is a grating module. The gratings are fanned within these modules to maintain a ~2.5° graze across the array given that the gratings intersect a focusing telescope beam. The 11° azimuthal span of each module leads to an overall telescope beam obscuration of 13%. Additional beam obscuration due to grating module structure (the belly bands) is less than 2%. Alignment of the grating module structure with the telescope structure may be able to reduce the additional obscuration from 2% to closer to 1%. The azimuthal span combined with the necessary radial coverage leads to grating widths ranging from 49-85 mm. The radial span of the gratings ranges from 0.257-0.444 m at the tower, thus necessitating 23 gratings per module for a total of 234 gratings. Projecting this radial coverage up to the telescope beam shows that the telescope radii responsible for feeding the OPXGS lie between 1.00-1.72 m. An overview of the module design is shown in Figure 10 and the characteristics of this design are given in Table 1.

OPXGS parameters	6 modules
Telescope mirror module	SPO, B4C coat, outer 35 rows, 10% loss, March 24 2010
Telescope beam obscuration (gratings)	13%
Telescope beam obscuration (structure)	0.3-2.0%
Grating module azimuthal coverage	11°
Grating module radial coverage (at the telescope)	1.00-1.72 m
Number of modules	6
Gratings per module	23
Grating mechanical throughput	93%
Grating graze angle	2.5°
Grating diffraction efficiency (no coating)	~90%
Reflective coating	Ir
Groove length	150 mm
Grating edge thickness	0.5 mm
CCD optical blocking filter thickness	28 nm Al, 13 nm MgF_2
Average effective area	1500 cm^2
Effective area @ 300 eV	1000 cm^2
Effective area contingency	30%

Table 1. Summary of the parameters describing the 6 module OP-XGS grating array.

An alternate view of the grating system, looking down the Z-axis from above the tower, is shown in Figure 11. This shows that the outer envelope of the tower at the position of the gratings is 1.0 m in diameter. This number has a minimum limit set by the size of the telescope beam at 5.16 m from the focus (~0.888 m diameter). At the lower end the three point mount for the tower hexapod rests on a 1.44 m diameter circle. These numbers are quite flexible, especially the location of the mounting feet, and therefore can be altered given changes in system interface requirements.

Furthermore, the positions of the gratings and camera are azimuthally independent and can be adjusted as necessary to facilitate accommodation at the instrument platform.

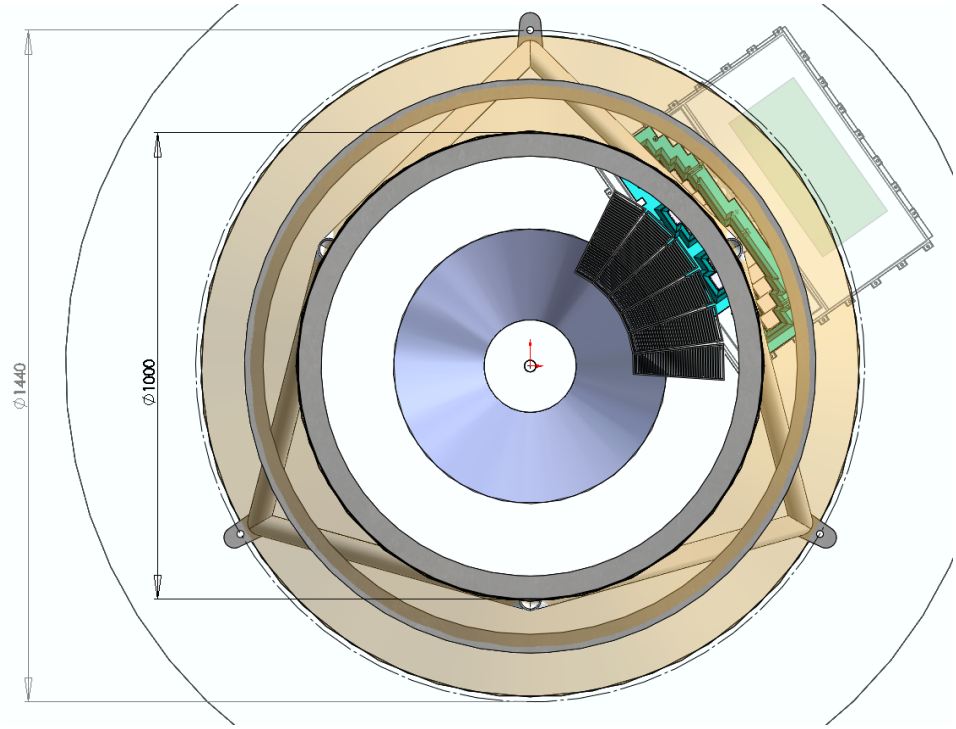

Figure 11. Grating system as viewed from FMA looking down towards array of 6 gratings mounted on the tower, with telescope main focus at center and CCD camera detecting diffracted beam.

The details on the design of the grating tower itself are presented in another paper, Casement et al.[10]

3.2 Grating thermal design

The operational temperature range is that in which the gratings must be maintained in order to achieve acceptable science performance. Thermal control is required on the OP-XGS grating array to reduce contamination due to condensation and to maintain the same temperature at which the system was pre-aligned. This is necessary because the thin gratings will be made of a structural material, beryllium, which has a moderate coefficient of thermal expansion (CTE). Internal components, such as the XGS, would be cold in the absence of heaters due to thermal blankets external to the spacecraft. The ±1 K requirement has been placed on the allowable gradient across a grating groove. The tolerance is looser in the cross dispersion direction. The ±1 K requirement is driven by maintaining flatness over the gratings in the pitch direction. A thermal design has been developed which can maintain a grating to grating temperature gradient of less than 15 mK at any given time and less than 350 mK over the IXO sun angle variation in the NGAS mission concept. This can be accomplished using less than 19 W power. This design incorporates Northrop Grumman approved, space qualified heaters and thermistors. A control board to run the heaters and thermistors is required and is housed in the camera electronics box.

Two basic thermal design configurations are currently under study. Configuration 1 uses conductive heating between the heaters and gratings and configuration 2 is a radiative heating method, which has reduced thermal gradients. Cable harnessing from the OP-XGS electronics box to the heaters and thermistors is lightweight and can be routed along the OP-XGS tower struts. All thermal modeling is preliminary, and checks incorporating the tower OP-XGS model into the

observatory Sinda model are pending. This concept can be used in any IXO architecture but may require more or less heater power, depending on the configuration, to maintain thermal gradients.

The design has been analyzed in a time-step, finite difference numerical thermal model which also takes into account IXO internal temperatures and sun angles. The analysis was originally performed using 4 grating modules but due to late changes in A_{eff} requirements upon OP-XGS it has been necessary to scale the outputs to correspond to the current baseline 6 module design. These scaled results are shown in Table 2 with a representative thermal control design shown in Figure 12.

Part	Quantity
NG Heaters	12
NG Thermistors	27
Grating Module Thermal Control Hardware (MLI / SLI)	1 set
Radiative Heater Panels	7
Cable Harness	1
Controller Board	1

Table 2. Analysis results for the basic thermal design configuration. The component budgets shown cover two possible design configurations; the quantity shown assumes the worst case (highest mass) scenario and is hence conservative.

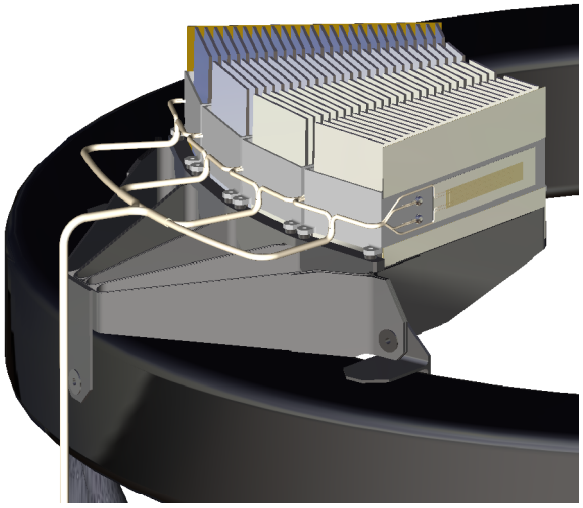

Figure 12. OP-XGS Grating Array with example thermal control hardware.

5. CONCLUSION

This paper presents findings from the ESA Instrument Study activities specific to the IXO OP-XGS concept. The results of this study are a robust grating system design. The system consists of an array of gratings, consisting of 6 identical modules held to a structural tower that places the grating array 5.16 m away from the CCD camera at the focal plane. This design was derived through a thorough analysis of how the concept achieves the performance requirements for the XGS: >1000 cm^2 effective area, spectral resolution > 3000, over the energy band 0.3-1.0 keV. Analyzing these factors in detail results in a baseline design that is capable of achieving an average of over 1500 cm^2 of effective area with spectral resolution ranging from 3600-7200 over the necessary energy band. This provides for significant margin in both requirements.

ACKNOWLEDGEMENTS

The authors would like to recognize and thank the support from NASA GSFC Cooperative Agreement NNX09AE51A.

REFERENCES

[1] McEntaffer, R. L., Murray, N. J., Holland, A. D., Lillie, C., Casement, S., Dailey, D., Johnson, T., Cash, W., Oakley, P., Schultz, T., Burrows, D. N., "Off-Plane Grating Spectrometer for the International X-ray Observatory," Proc. SPIE 7437, 74370H-74370H-13, (2009).

[2] McEntaffer, R. L., Murray, N. J., Holland, A., D., Lillie, C., Casement, S., Dailey, D., Johnson, T., Cash, W., Oakley, P., "Off-plane X-ray grating spectrometer for the International X-ray Observatory," Proc. SPIE 7360, 73600H-73600H-11, (2009).

[3] Casement, S., Johnson, T, Lillie, C., McEntaffer, R. L., Cash, W., "The Off-Plane X-ray Grating Spectrometer for the International X-ray Observatory," Bulletin of the AAS 42, 572, (2010).

[4] Cash, W., McEntaffer, R. L., Casement, S., "Optical Designs for the Off-plane Spectrograph on the International X-ray Observatory," Bulletin of the AAS 41, 722, (2010).

[5] Cash, W. C., "X-ray optics. 2: A technique for high resolution spectroscopy," Applied Optics, 30, 1749, (1991).

[6] Murray, N. J., Holland, A. D., Tutt, J., Evagora, A., Barber, S. J., Pool, P., Endicott, J., Burt, D., Walton, D. M., Page, M., McEntaffer, R. L., Cash, W., Lillie, C., Casement, S., "Off-plane x-ray grating spectrometer camera for IXO," Proc. SPIE 7742, 7742-95, (2010).

[7] Holland, A. D., Murray, N. J., Tutt, J., McEntaffer, R. L., Pool, P., Endicott, J., "CCD readout for the IXO off-plane grating spectrometer," Proc. SPIE 7435, 74350Y-74350Y-9, (2009).

[8] Tutt, J., Holland, A. D., Murray, N. J., Hall, D. J., McEntaffer, R. L., Endicott, J., Robbins, M., "A study of Electron-Multiplying CCDs for use on the International X-ray Observatory Off-Plane X-ray Grating Spectrometer," Proc SPIE 7742, 7742-33, (2010).

[9] Casement, S., McEntaffer, R. L., Cash, W., Johnson, T., Lillie, C., "A Tower Concept for the Off-Plane X-ray Grating Spectrometer for the International X-ray Observatory," Bulletin of the AAS, 41, 739, (2010).

[10] Casement, S., McEntaffer, R. L., Cash, W., Johnson, T., Lillie, C., "A Tower Concept for the Off-Plane X-ray Grating Spectrometer for the International X-ray Observatory," Proc. SPIE 7732, 7732-140, (2010).